Published in final edited form as:
J Nucl Med. 2014 September ; 55(9): 1438–1444. doi:10.2967/jnumed.114.141093.

Absolute Quantitation of Myocardial Blood Flow in Human Subjects with or without Myocardial Ischemia using Dynamic Flurpiridaz F 18 Positron Emission Tomography

René R. S. Packard[1], **Sung-Cheng Huang**[2], **Magnus Dahlbom**[2], **Johannes Czernin**[2], and **Jamshid Maddahi**[1,2]

[1]Department of Medicine (Cardiology), Ronald Reagan UCLA Medical Center, University of California, Los Angeles

[2]Department of Molecular and Medical, Pharmacology (Nuclear Medicine), Ronald Reagan UCLA Medical Center, University of California, Los Angeles

Abstract

Absolute quantitation of myocardial blood flow (MBF) by positron emission tomography (PET) is an established method of analyzing coronary artery disease (CAD) but subject to the various shortcomings of available radiotracers. Flurpiridaz F 18 is a novel PET radiotracer which exhibits properties of an ideal tracer.

Methods—A new absolute perfusion quantitation method with Flurpiridaz was developed, taking advantage of the early kinetics and high first-pass extraction by the myocardium of this radiotracer, and the first in human measurements of MBF performed in 7 normal subjects and 8 patients with documented CAD. PET images with time-activity curves were acquired at rest and during adenosine stress.

Results—In normal subjects, regional MBF between coronary artery territories did not differ significantly, leading to a mean global MBF of 0.73 mL/min/g at rest and 2.53 mL/min/g during stress, with a mean global myocardial flow reserve (MFR) of 3.70. CAD vascular territories with <50% stenosis demonstrated a mean MBF of 0.73 at rest and 2.02 during stress, leading to a mean MFR of 2.97. CAD vascular territories with ≥50% stenosis exhibited a mean MBF of 0.86 at rest and 1.43 during stress, leading to a mean MFR of 1.86. Differences in stress MBF and MFR between normal and CAD territories, as well as between <50% and ≥50% stenosis vascular territories, were significant ($P<0.01$).

Conclusion—Absolute quantitation of MBF in humans with the novel PET radiotracer Flurpiridaz is feasible over a wide range of cardiac flow in the presence or absence of stress-inducible myocardial ischemia. The significant decrease in stress MBF and ensuing MFR in CAD territories allows a clear distinction between vascular territories exhibiting stress-inducible myocardial ischemia and those with normal perfusion.

Corresponding author: Jamshid Maddahi, MD, Department of Medicine (Cardiology) and Department of Molecular and Medical Pharmacology (Nuclear Medicine), Ronald Reagan UCLA Medical Center, University of California, Los Angeles. 757 Westwood Boulevard, 100 Medical Plaza, Suite 410, Los Angeles, CA 90095. Phone: 310-889-0769. jmaddahi@mednet.ucla.edu.

DISCLOSURE

The other authors have no potential conflicts of interest to disclose.

Keywords

Flurpiridaz; PET; MBF; MFR; Human

INTRODUCTION

Absolute quantitation of myocardial blood flow (MBF) by positron emission tomography (PET) has a significant role in the clinical evaluation of epicardial and microvascular coronary artery disease (CAD) (1). Although the clinical value of the absolute quantitation of MBF by PET is well recognized, this technique is not often used due to limitations of currently available radiotracers (2).

PET radiotracers such as Rb82 chloride, N13 ammonia, and O15 water have been utilized to quantitate absolute MBF. Due to their short half-lives, O15 is limited to facilities with an onsite cyclotron whereas N13 requires either an onsite or nearby cyclotron. Rb82 is generator-produced and is approved for the clinical assessment of myocardial perfusion. However, its very short half-life affects image quality with noisy time-activity curves (TAC) reducing the tracer's ability to quantify myocardial perfusion. A desirable myocardial perfusion agent should have a very high first-pass extraction fraction and track regional MBF over a wide range, permitting accurate determination of absolute MBF. The agent should exhibit excellent target-to-non-target uptake ratios, with high uptake in the myocardium and low uptake or rapid clearance from adjacent organs. Furthermore, it should be available as a unit dose from regional cyclotrons, obviating the need for on-site cyclotrons or costly Rb82 generators (2).

Flurpiridaz is a novel PET myocardial perfusion imaging (MPI) agent labeled with F 18. It is a structural analog of the insecticide pyridaben, a known inhibitor of the NADH:ubiquinone oxidoreductase also known as mitochondrial complex-1 (MC-1) of the electron transport chain (3). Flurpiridaz inhibits MC-1 by competing for binding with ubiquinone without affecting the viability of cardiomyocytes. This radiotracer exhibits a rapid uptake and slow washout from cardiomyocytes (3). Experimental PET imaging demonstrates a high and sustained cardiac uptake which is proportional to blood flow (4). In rats, the first-pass extraction fraction of Flurpiridaz by the myocardium is 94% (5). The flow-independent extraction fraction of Flurpiridaz implies a linear relationship between uptake and MBF, an important attribute for stress MBF measurements (5). In a pig model, Flurpiridaz exhibits higher activity ratios of the myocardium vs. the blood, liver and lungs compared to N13 ammonia (6). Moreover, Flurpiridaz has an excellent correlation with radioactive microspheres in assessing absolute quantitation of regional MBF over flow ranges from 0.1 – 3.0 mL/min/g (6) (7). This radiotracer also permits evaluation of myocardial infarction size in rats (8). Importantly, the isotope F 18 has a 110min half-life, making delivery of unit doses from regional cyclotrons feasible.

Use of this compound in human studies (2) (9) (10) demonstrated excellent quality myocardial images in addition to exhibiting many desirable properties of an ideal myocardial perfusion tracer including high myocardial uptake, slow myocardial clearance, and high myocardial-to-background contrast (3) (4) (5). In the present study, we sought to

perform the absolute quantitation of MBF and derive the MFR using this compound in a group of normal subjects and CAD patients.

Methods to use Flurpiridaz for the quantitation of myocardial perfusion have been proposed and validated in a pig model (6) in which a 2-tissue compartmental model was used to fit myocardial kinetics of 10 or 20 minutes and to estimate myocardial perfusion. The modeling approach was similar to the one for N13 ammonia cardiac PET studies, except labeled metabolites in the blood were ignored and the tracer binding deemed irreversible. This approach is susceptible to potential variations in labeled metabolites in the blood and subject movement which is a major concern with the high spatial imaging resolution of current PET/CT scanners. Others proposed using a static scan to simplify the quantitation procedure (7). They found that in the pig model the MFR obtained with the static scan approach matched the value obtained with microspheres, provided the scan time is from 5 to 10 min and the value is normalized by the blood pool activity in the 0 to 3 min image. The approach, however, still required the subject to be scanned starting with tracer injection time, and it did not provide accurate values for MBF.

In this study, we employ a quantitation method that can provide quantitative MBF using Flurpiridaz F 18. The method utilizes the early kinetics of myocardial uptake of the tracer. It takes advantage of the high first-pass extraction fraction of the tracer (5), i.e. no compartmental modeling is required and is less dependent on the assumptions necessitated by other proposed approaches discussed above. Since the method depends only on the dynamic images of a very short early time (less than two minutes), it is not as sensitive to subject movements. The method was applied both to normal subjects with low likelihood of myocardial ischemia and CAD patients with stress-inducible myocardial ischemia.

MATERIALS AND METHODS

Human Subject/Patient Selection, Preparation Of Flurpiridaz F 18 and Statistical Analysis can be found in the Supplements section.

PET Imaging Procedures

Two Flurpiridaz PET imaging sessions were performed in each subject/patient. The first was done at rest, and either on the same day or the following day, the PET imaging was repeated under stress with adenosine infused at a rate of 140 mcg/kg body weight/min for 6 minutes, starting at 3 minutes before the injection of the tracer. 11 of the PET studies (6 normal and 5 CAD) were done using a same-day protocol, and 4 (1 normal and 3 CAD) were done using a 2-day protocol. For the same day studies, the rest study was performed first, and the stress study was performed 52.9 ± 11.2min later, as previously reported (10). At 60min after the rest injection, the tracer distribution in the heart did not change much over a 5min period, and the TAC values measured before the stress injection were averaged and subtracted from the stress TAC before the modeling analysis was performed. There was no significant increase in noise in the TACs when using the subtraction procedure in the same-day protocol as compared with the 2-day protocol. For each imaging session, the subject was positioned supine in a PET/CT scanner (Biograph 64, Siemens Inc.). Following CT imaging of the chest, Flurpiridaz (5 mCi) was administered IV as a slow bolus over 10 sec followed

by a 5–10 mL saline flush. PET imaging was started concomitantly to Flurpiridaz injection and list mode data were collected for 10 minutes. Thereafter, the list mode data were framed into a scan sequence of 12×10, 4×30, 1×60, and 1×300 sec. Images were reconstructed using a 2D OSEM iterative algorithm (8 subsets and 21 iterations). No post reconstruction filtering was applied, resulting in a spatial resolution of 6.5 mm FWHM (full width at half maximum).

Image Analysis

The dynamic transaxial images were first reoriented into short axis slices. These were then used to produce dynamic polar maps, where the sampling points were defined on a 6 minute summed framed at the end of the acquisition. Regions of Interest (ROI) corresponding to the three coronary territories were defined on the dynamic polar maps. A polar map was used to normalize the size and shape of hearts from different individuals and allow ROI to be obtained more consistently and objectively. Using these ROI, tissue time-activity-curves (TACs) were generated from the dynamic polar maps. A blood pool TAC was generated by placing a small ROI in the center of the left ventricle of the last frame of the dynamic short axis images. This procedure was applied to both the rest and stress data (11).

Absolute Quantitation Of Myocardial Blood Flow

Quantitative myocardial perfusion in each perfusion territory was estimated using the tracer uptake kinetics within the first 90 seconds post tracer injection. Within this period, the tracer was assumed to be taken up by the myocardium without significant clearance, and with very few if any labeled metabolites contained in the blood during this early time period. Therefore, the radioactivity concentration in myocardial segment i can be described by Eq. 1 below.

$$C_i(t)=F_i\int_0^t C_p(\tau)d\tau+V_{bi}C_p(t), \text{for} i=1,2,3 \quad \text{Eq. 1}$$

where the subscripts i=1, 2, and 3 indicate, respectively, the myocardial activities in the three perfusion territories (i.e., LAD, LCx, RCA), $C_p(t)$ is the radioactivity concentration in blood, and V_{bi} is the vascular volume in that myocardial segment. Due to the partial volume effect and the spillover of activities between myocardium and blood pool, the measured radioactivity concentration in the blood pool ($C_p(t)$) and in the myocardial regions of the three perfusion territories ($C_i(t)$, for i=1,2,3) from the dynamic PET images can be described by the following equations.

$$C_p(t)_{measured}=RC_{bp}\times C_p(t)+\sum_{i=1}^{3}SPF_{mbi}\times C_i(t)$$

$$C_i(t)_{measured}=RC_i\times C_i(t)+SPF_{bmi}\times C_p(t), \text{for} i=1,2,3 \quad \text{Eq, 2}$$

$$=RC_i \times F_i \int_0^t C_p(\tau)d\tau + (V_b + SPF_{bmi}) \times C_p(t), \text{for} i=1,2,3$$

where RC is the recovery coefficient due to the partial volume effect (of the myocardium or the blood pool); SPF is the spillover fraction (the subscript bmi denotes the spillover from blood pool to myocardium region i, and mbi denotes the spillover fraction from myocardium segment i to the blood pool ROI).

Equation 2 was used to fit the measured myocardial TACs. With the approximation that RC_{bp} = 0.95 and SPF_{mbi} = 0.05/3 (i=1, 2, and 3), blood pool TAC ($C_p(t)$) was calculated from the measured blood pool TAC and the myocardial TACs directly, as

$$C_p(t) = \frac{1}{RC_{bp}} \times [C_p(t)_{measured} - \sum_{i=1}^{3} SPF_{mbi} \times C_i(t)] \quad \text{Eq. 3}$$

$$= \frac{1}{0.95} \times [C_p(t)_{measured} - \sum_{i=1}^{3} (0.05/3) \times C_i(t)]$$

Furthermore, the spillover fraction from blood pool to myocardium plus the vascular volume was approximated as 1.0 minus the RC of the corresponding myocardial segment. That is,

$$(\mathrm{SPF_{bmi}} + \mathrm{V_{bi}}) = 1.0 - \mathrm{RC_i} \text{for} i=1,2, \text{and} 3. \quad \text{Eq. 4}$$

An iterative procedure in which the measured TAC of each perfusion territory was regressed one at a time, with the estimated $C_p(t)$ fixed from a previous iteration. After each round of regression of the measured TACs of the three perfusion territories, $C_p(t)$ was updated (with Eq. 3). The procedure was then repeated. Usually, the estimated values of F_i and RC_i converged within ~3 iterations.

Global myocardial perfusion ($C_g(t)_{measured}$) was estimated from the weighted average of the TACs of the three territories (weighted by their approximate areas on the polar map). That is,

$$\mathrm{C_g(t)_{measured}} = (7\mathrm{C_1(t)_{measured}} + 5\mathrm{C_2(t)_{measured}} + 5\mathrm{C_3(t)_{measured}})/17. \quad \text{Eq. 5}$$

The equation used for estimating the global myocardial perfusion is the same as those for each myocardial segment (i.e., Eq. 2), except that the $C_p(t)$ estimated at the end of the regression for individual myocardial segment was used for estimating the global myocardial perfusion.

After F_i was determined, myocardial blood flow (MBF) was obtained by assuming a first-pass extraction fraction of 0.94 (5). That is,

$$MBF_i = F_i / 0.94. \quad \text{Eq. 6}$$

The units of MBF_i are in (mL of blood)/min/(g of myocardium), assuming that the specific density of myocardium is ~ 1.0 g/mL. Since the kinetic data were corrected for partial volume, spillover, and vascular activity, the MBF value obtained corresponded to the blood perfusion value in myocardium with blood in the vasculature removed.

Calculation of Myocardial Flow Reserve

Myocardial flow reserve for each myocardial segment was calculated as the ratio of the segment's MBF value with adenosine infusion to the MBF value at rest.

$$MFR = (MBF \text{during adenosine infusion}) / (MBF \text{at rest}) \quad \text{Eq. 7}$$

RESULTS

A representative polar map depicting relative perfusion in a CAD patient with stress-inducible ischemia is shown, demonstrating a reversible defect mostly in the LAD distribution (Figure 1).

The tracer kinetics in a normal myocardial region along with the blood pool time-activity curve (TAC) is illustrated (Figure 2). The model fitted curves at the end of the MBF estimation are also shown.

The MBF in each vascular territory of normal subjects with low likelihood of myocardial ischemia under rest and stress conditions with ensuing myocardial flow reserve is depicted as means ± standard deviations (Figure 3). There were no significant differences in flow between the LAD, LCx and RCA territories in each condition, with P-values of 0.70 for resting myocardial blood flow (RMBF), 0.11 for stress myocardial blood flow (SMBF) and 0.99 for MFR. For each vascular territory, there was a significant difference between RMBF and SMBF, RMBF and MFR, SMBF and MFR with P-values < 0.001.

The regional MBF in the LAD, LCx and RCA territories as well as global MBF derived from weighted contributions from each vascular territory (Eq. 5) in normal subjects with low likelihood of myocardial ischemia compared to regional MBF in < 50% stenosis and ≥ 50% stenosis vascular territories is detailed (Table 2). In low likelihood territories, mean ± standard deviation of global MBF was 0.73 ± 0.13 mL/min/g at rest and 2.53 ± 0.48 mL/min/g at stress, leading to a MFR of 3.70 ± 0.39. In < 50% stenosis vascular territories, mean ± standard deviation of MBF was 0.73 ± 0.09 at rest and 2.02 ± 0.40 at stress, leading to a MFR of 2.97 ± 0.76. In ≥ 50% stenosis vascular territories, mean ± standard deviation of MBF was 0.86 ± 0.21 mL/min/g at rest and 1.43 ± 0.31 mL/min/g at stress, leading to a MFR of 1.86 ± 0.59. There was no significant difference in rest MBF in global or regional vascular flow between the low likelihood and < 50% stenosis (P=0.97) or ≥ 50% stenosis (P=0.73) vascular territories. Differences in stress MBF (P=0.004) and MFR (P=0.003) between global flow in low likelihood and <50% vascular territories were significant. Similarly, differences in stress MBF (P=0.001) and MFR (P=0.001) between global flow in

low likelihood and ≥ 50% vascular territories were significant. Differences were also significant when comparing individual vascular territories from normal subjects to individual vascular territories with < 50% stenosis or ≥ 50% stenosis from CAD patients (data not shown). Finally, comparing < 50% stenosis to ≥ 50% stenosis vascular territories, there was no significant difference in rest MBF (P=0.073) but there was a significant difference in stress MBF (P<0.001) and MFR (P<0.001).

The regional MBF and MFR in the vascular territories of normal subjects with low likelihood of myocardial ischemia (n=21 territories) vs. the vascular territories of CAD patients with < 50% stenosis (n=12 territories) and ≥ 50% stenosis (n=12 territories) is illustrated further and presented as means ± standard deviations (Figure 4). There was no significant difference in RMBF between conditions. As detailed above, SMBF and MFR was significant when comparing low likelihood to < 50% stenosis, low likelihood to ≥ 50% stenosis and < 50% stenosis to ≥ 50% stenosis vascular territories.

The scatterplot of the MFR obtained from each individual territory in normal subjects with low likelihood of myocardial ischemia compared to < 50% stenosis and ≥ 50% stenosis territories in CAD patients is illustrated in detail (Figure 5). Horizontal bars represent the respective mean values: 3.70 in low likelihood, 2.97 in < 50% stenosis and 1.86 in ≥ 50% stenosis. Differences were significant when comparing the MFR from low likelihood to < 50% stenosis (P=0.003), low likelihood to ≥ 50% stenosis (P=0.001) and < 50% stenosis to ≥ 50% stenosis vascular territories (P<0.001).

DISCUSSION

The present study is the first in human analysis of the absolute quantitation of MBF using Flurpiridaz PET. Analyses were performed in both normal subjects and CAD patients providing MBF data over a wide range of conditions. The importance of the absolute quantitation of MBF and its prognostic implication in the presence of abnormal MFR has been previously established. O15 water PET accurately detects CAD (12) and N13 ammonia MFR has a strong association with prognosis (13) (14). Rb82 MBF and MFR correctly detects 3-vessel CAD (15) and predicts adverse cardiovascular events (16) beyond relative MPI and the sum stress score (17). Moreover, absolute quantitation of MBF with Rb82 is an independent predictor of cardiac mortality in patients with known or suspected CAD and provides incremental risk stratification over established clinical variables and relative MPI (18).

Flurpiridaz exhibits many advantages over existing PET radiotracers, and meets the conditions of an ideal perfusion tracer (2). Flurpiridaz has a high extraction fraction by the myocardium, a short positron range providing high-resolution images, and a relatively long half-life of 110 minutes allowing it to be produced at regional cyclotrons. This novel PET radiotracer is compatible with both pharmacological and exercise stress imaging.

The present study demonstrates the feasibility of absolute quantitation of MBF with Flurpiridaz. All MBF quantitation processes involve some assumptions, with potential errors introduced cancelling out when calculating MFR. Previous reference values using

established PET radiotracers reported a rest MBF of 0.62 – 0.92 mL/min/g and a stress MBF of 1.97 – 3.55 mL/min/g in normal subjects, usually leading to a MFR of 3.5 – 4.0. Patients with CAD display a significantly lower stress MBF typically leading to a MFR of 2.0 – 2.5 in borderline abnormal studies and < 2.0 in frankly abnormal studies (1). MFR cutoffs for abnormal studies vary somewhat depending on the radiotracer used as well as the reference gold standard (fractional flow reserve during cardiac catheterization or ≥ 50% vs. ≥ 70% diameter stenosis during angiography) (19).

Since no reference standard was used in the present study, the accuracy of the quantitation values reported is subject to caution. The population was too small to use invasive angiography as a reference standard. Given the 94% myocardial extraction of Flurpiridaz, we anticipate our absolute MBF quantitation results will correlate best with MBF values obtained with N13 ammonia and O15 water which exhibit high extraction fractions of 80% and 100%, respectively, and have robust MBF reproducibility (1). We expect less correlation however with Rb82 chloride due to its lower (65%) and sigmoid-shaped extraction at elevated myocardial blood flows necessitating software correction (20). Future studies will be conducted to provide values of absolute myocardial blood flow and ensuing myocardial flow reserve with cutoffs below which the presence of CAD, whether epicardial or microvascular, may be predicted in a clinically useful manner.

Importantly, regional perfusion and myocardial uptake measurements are feasible with Flurpiridaz PET imaging. In normal subjects, a uniformity of MBF was observed at rest and during adenosine stress in the LAD, LCx and RCA territories. Similar results have been observed with other radiotracers (21) (22).

Interestingly, CAD vascular segments with <50% stenosis exhibited stress MBF and MFR values between those from vascular segments with ≥50% stenosis and those from normal subjects. Consistent with previous reports, this suggests that despite being labeled as angiographically non-significant, these territories are not normal and exhibit hemodynamic and metabolic abnormalities. Previously suggested mechanisms include abnormalities of endothelium-dependent and/or smooth muscle cell-dependent vasomotion, with these patients being at increased risk of future cardiovascular events (1).

The MBF quantitation procedure we adopted only uses the Flurpiridaz kinetics of the first 1.5 minutes. The procedure does not require taking blood samples from the patients to provide the input function, and thus does not need cross-calibration of the PET measurement with other devices such as well counters that frequently introduce large errors in practical situations. The procedure is based on a few assumptions that are supported by known kinetics of Flurpiridaz in blood and myocardium. First, it assumes that within the first 1.5 minutes post tracer injection there are few if any F 18 labeled metabolites in the blood. This is supported by results in animal and human studies. Another assumption is that, after myocardial uptake of Flurpiridaz, the compound is not cleared from the myocardium in a significant amount within 1.5 minutes. This is corroborated by animal and human studies demonstrating that the clearance rate constant of the compound in the myocardium was measured in hours (3) (4) (5) (6) (9) and no additional clearance component (e.g., due to the interstitial space) of faster clearance rate was observed in the kinetics of the first-pass

extraction fraction measurements (5). Thus the modeling of the myocardial uptake of Flurpiridaz as an irreversible process (Eq. 1) is quite valid. The two assumptions made here were also made by Sherif et al (7) in their calculations of MFR and the tracer retentions in the myocardium of pig models, except that they calculated the retentions using a longer period of scan time (5–10 min for myocardial activity and 0–3 min for area under the blood TAC). The longer times made the assumptions less valid. Although the errors created were somewhat cancelled when calculating the MFR (as a ratio of stress and rest retentions), the retention measurements they obtained did not correlate well with the MBF determined by microspheres.

Another reason for their retention measurements failing to match the microsphere-measured perfusion is that their retention measurements did not consider partial volume and spillover effects in their calculations. In the procedure used in the present study, the partial volume effect and spillover of activities were explicitly accounted for (Eq. 2), although some assumptions and approximations (Eqs. 3 and 4) were employed to simplify the procedure and make the estimation of myocardial perfusion more tractable and robust. The approach proposed by Nekolla et al (6) using a 2-tissue compartment did account for the partial volume effect and spillover fraction similar to our procedure. However, their approach using ten or twenty minutes of kinetics (0–10 or 0–20 min) is susceptible to subject movement during the imaging time that is difficult to avoid, especially for stress studies. Also, the assumption of having negligible labeled metabolites in the blood is no longer valid for Flurpiridaz over such a long time period.

A potential disadvantage of using short kinetics to quantitate perfusion is the lack of adequate count statistics to give a reliable assessment, such as with Rb82 determined MBF. However, due to the high first-pass extraction fraction of Flurpiridaz by the myocardium, the dynamic PET images of the heart in the first 2 minutes were of adequate quality and allowed measuring kinetics in myocardial regions well (Fig. 2). The use of modeling fitting to the measured kinetics rather than just using a single integrated value also maximizes the value of the available data for estimation of myocardial perfusion. In the current study, the relative small variability of the MBF estimates obtained under both rest and stress conditions in normal subjects and in the myocardial segments of <50% stenosed CAD patients clearly demonstrate the stability of the measurements based on the 1.5-min short kinetics and support the robustness of the quantitation procedure used.

In our MBF quantitation procedure, we also used a fixed value of 0.94 for the first-pass extraction fraction. This first-pass extraction fraction value was previously determined in a Langendorff preparation of rat heart (5) and was found to be independent of perfusion flow. Although the first-pass extraction fraction was taken directly from an animal study, its use in the present study gives human MBF values comparable to the commonly accepted values obtained by other methods. Even though the extraction fraction in humans may deviate slightly from 0.94, the resulting MBF would not change significantly. In addition, a high first-pass extraction fraction is not significantly dependent on perfusion, and hence the conversion of tracer uptake to MBF can be greatly simplified (Eq. 6).

Certain aspects of the current MBF quantitation procedure, however, can be further improved to make it more useful in the clinical setting. For example, the extension of the method for generating MBF parametric images could take the quantitation to a level usable for routine clinical studies. Subsequent studies will measure MBF over finer coronary segments such as the standardized 17-segment left ventricular myocardial model which may be of greater clinical use. In the present study, normal subjects were recruited on the basis of their low likelihood of having myocardial ischemia. Given the presence of classic cardiovascular risk factors (Table 1) in this group, and despite their absence of angina, anginal equivalent or evidence of stress-inducible ischemia by electrocardiogram or PET MPI, this group may have had subclinical coronary artery disease. This may theoretically have led the stress MBF in the group of normal subjects to be lower than in a group of young subjects with complete absence of cardiovascular risk factors which were not included in the present study. Also, comparison of MBF measurements obtained through Flurpiridaz with those currently accepted using N13 ammonia PET in the same subjects is expected to provide further validation or improvement of the quantitative MBF method reported in this study, e.g. confirmation of the first-pass extraction fraction of 0.94.

CONCLUSION

Using a robust perfusion quantitation procedure, absolute quantitation of MBF using Flurpiridaz F 18 cardiac PET imaging is feasible in both normal subjects with low likelihood of myocardial ischemia and CAD patients. No significant differences in MBF (either at rest or with adenosine stress) and MFR were found among the three coronary perfusion territories in subjects with no stress-inducible ischemia. In CAD patients, diseased vascular segments had significantly lower MBF in response to adenosine stress and thus a reduced MFR. Future studies will determine cutoff values for stress MBF and MFR in patients with CAD for direct clinical applicability. We believe patient risk stratification using PET imaging will be feasible in a broad clinical setting both by utilizing relative perfusion as well as through the absolute quantitation of MBF. These initial results suggest that Flurpiridaz, which is not yet approved by the United States Food and Drug Administration as a PET MPI agent, is uniquely poised as a radiotracer to fulfill all these requirements.

Supplementary Material

Refer to Web version on PubMed Central for supplementary material.

ACKNOWLEDGEMENTS

The authors are indebted to James Sayre, PhD from the UCLA Department of Biostatistics who performed the statistical analyses. The authors are also grateful to John Williams and David Truong for their expert technical assistance.

FUNDING

The phase II clinical trial analyzing Flurpiridaz MPI was sponsored by Lantheus Medical Imaging. Lantheus Medical Imaging had no role in the design of this study, analysis of its data or writing of the manuscript. Dr. Packard is supported by NIH grant T32 HL007895. Dr. Maddahi is supported by a research grant from Lantheus Medical Imaging.

Dr. Maddahi is a scientific advisor to Lantheus Medical Imaging.

REFERENCES

1. Schindler TH, Schelbert HR, Quercioli A, Dilsizian V. Cardiac PET imaging for the detection and monitoring of coronary artery disease and microvascular health. JACC Cardiovascular imaging. 2010 Jun; 3(6):623–640. [PubMed: 20541718]
2. Maddahi J. Properties of an ideal PET perfusion tracer: new PET tracer cases and data. Journal of nuclear cardiology : official publication of the American Society of Nuclear Cardiology. 2012 Feb; 19(Suppl 1):S30–S37. [PubMed: 22259007]
3. Yalamanchili P, Wexler E, Hayes M, et al. Mechanism of uptake and retention of F-18 BMS-747158-02 in cardiomyocytes: a novel PET myocardial imaging agent. Journal of nuclear cardiology : official publication of the American Society of Nuclear Cardiology. 2007 Nov-Dec; 14(6):782–788. [PubMed: 18022104]
4. Yu M, Guaraldi MT, Mistry M, et al. BMS-747158-02: a novel PET myocardial perfusion imaging agent. Journal of nuclear cardiology : official publication of the American Society of Nuclear Cardiology. 2007 Nov-Dec;14(6):789–798. [PubMed: 18022105]
5. Huisman MC, Higuchi T, Reder S, et al. Initial characterization of an 18F-labeled myocardial perfusion tracer. Journal of nuclear medicine : official publication, Society of Nuclear Medicine. 2008 Apr; 49(4):630–636.
6. Nekolla SG, Reder S, Saraste A, et al. Evaluation of the novel myocardial perfusion positron-emission tomography tracer 18F-BMS-747158-02: comparison to 13N-ammonia and validation with microspheres in a pig model. Circulation. 2009 May 5; 119(17):2333–2342. [PubMed: 19380625]
7. Sherif HM, Nekolla SG, Saraste A, et al. Simplified quantification of myocardial flow reserve with flurpiridaz F 18: validation with microspheres in a pig model. Journal of nuclear medicine : official publication, Society of Nuclear Medicine. 2011 Apr; 52(4):617–624.
8. Sherif HM, Saraste A, Weidl E, et al. Evaluation of a novel (18)F-labeled positron-emission tomography perfusion tracer for the assessment of myocardial infarct size in rats. Circulation Cardiovascular imaging. 2009 Mar; 2(2):77–84. [PubMed: 19808572]
9. Maddahi J, Czernin J, Lazewatsky J, et al. Phase I, first-in-human study of BMS747158, a novel 18F-labeled tracer for myocardial perfusion PET: dosimetry, biodistribution, safety, and imaging characteristics after a single injection at rest. Journal of nuclear medicine : official publication, Society of Nuclear Medicine. 2011 Sep; 52(9):1490–1498.
10. Berman DS, Maddahi J, Tamarappoo BK, et al. Phase II safety and clinical comparison with single-photon emission computed tomography myocardial perfusion imaging for detection of coronary artery disease: flurpiridaz F 18 positron emission tomography. Journal of the American College of Cardiology. 2013 Jan 29; 61(4):469–477. [PubMed: 23265345]
11. Schindler TH, Zhang XL, Vincenti G, et al. Diagnostic value of PET-measured heterogeneity in myocardial blood flows during cold pressor testing for the identification of coronary vasomotor dysfunction. Journal of nuclear cardiology : official publication of the American Society of Nuclear Cardiology. 2007 Sep-Oct;14(5):688–697. [PubMed: 17826322]
12. Kajander S, Joutsiniemi E, Saraste M, et al. Cardiac positron emission tomography/computed tomography imaging accurately detects anatomically and functionally significant coronary artery disease. Circulation. 2010 Aug 10; 122(6):603–613. [PubMed: 20660808]
13. Tio RA, Dabeshlim A, Siebelink HM, et al. Comparison between the prognostic value of left ventricular function and myocardial perfusion reserve in patients with ischemic heart disease. Journal of nuclear medicine : official publication, Society of Nuclear Medicine. 2009 Feb; 50(2): 214–219.
14. Herzog BA, Husmann L, Valenta I, et al. Long-term prognostic value of 13N-ammonia myocardial perfusion positron emission tomography added value of coronary flow reserve. Journal of the American College of Cardiology. 2009 Jul 7; 54(2):150–156. [PubMed: 19573732]
15. Parkash R, deKemp RA, Ruddy TD, et al. Potential utility of rubidium 82 PET quantification in patients with 3-vessel coronary artery disease. Journal of nuclear cardiology : official publication of the American Society of Nuclear Cardiology. 2004 Jul-Aug;11(4):440–449. [PubMed: 15295413]

16. Fukushima K, Javadi MS, Higuchi T, et al. Prediction of short-term cardiovascular events using quantification of global myocardial flow reserve in patients referred for clinical 82Rb PET perfusion imaging. Journal of nuclear medicine : official publication, Society of Nuclear Medicine. 2011 May; 52(5):726–732.

17. Ziadi MC, Dekemp RA, Williams KA, et al. Impaired myocardial flow reserve on rubidium-82 positron emission tomography imaging predicts adverse outcomes in patients assessed for myocardial ischemia. Journal of the American College of Cardiology. 2011 Aug 9; 58(7):740–748. [PubMed: 21816311]

18. Murthy VL, Naya M, Foster CR, et al. Improved cardiac risk assessment with noninvasive measures of coronary flow reserve. Circulation. 2011 Nov 15; 124(20):2215–2224. [PubMed: 22007073]

19. Johnson NP, Gould KL. Integrating noninvasive absolute flow, coronary flow reserve, and ischemic thresholds into a comprehensive map of physiological severity. JACC Cardiovascular imaging. 2012 Apr; 5(4):430–440. [PubMed: 22498334]

20. Saraste A, Kajander S, Han C, Nesterov SV, Knuuti J. PET: Is myocardial flow quantification a clinical reality? Journal of nuclear cardiology : official publication of the American Society of Nuclear Cardiology. 2012 Oct; 19(5):1044–1059. [PubMed: 22733534]

21. Czernin J, Muller P, Chan S, et al. Influence of age and hemodynamics on myocardial blood flow and flow reserve. Circulation. 1993 Jul; 88(1):62–69. [PubMed: 8319357]

22. Nagamachi S, Czernin J, Kim AS, et al. Reproducibility of measurements of regional resting and hyperemic myocardial blood flow assessed with PET. Journal of nuclear medicine : official publication, Society of Nuclear Medicine. 1996 Oct; 37(10):1626–1631.

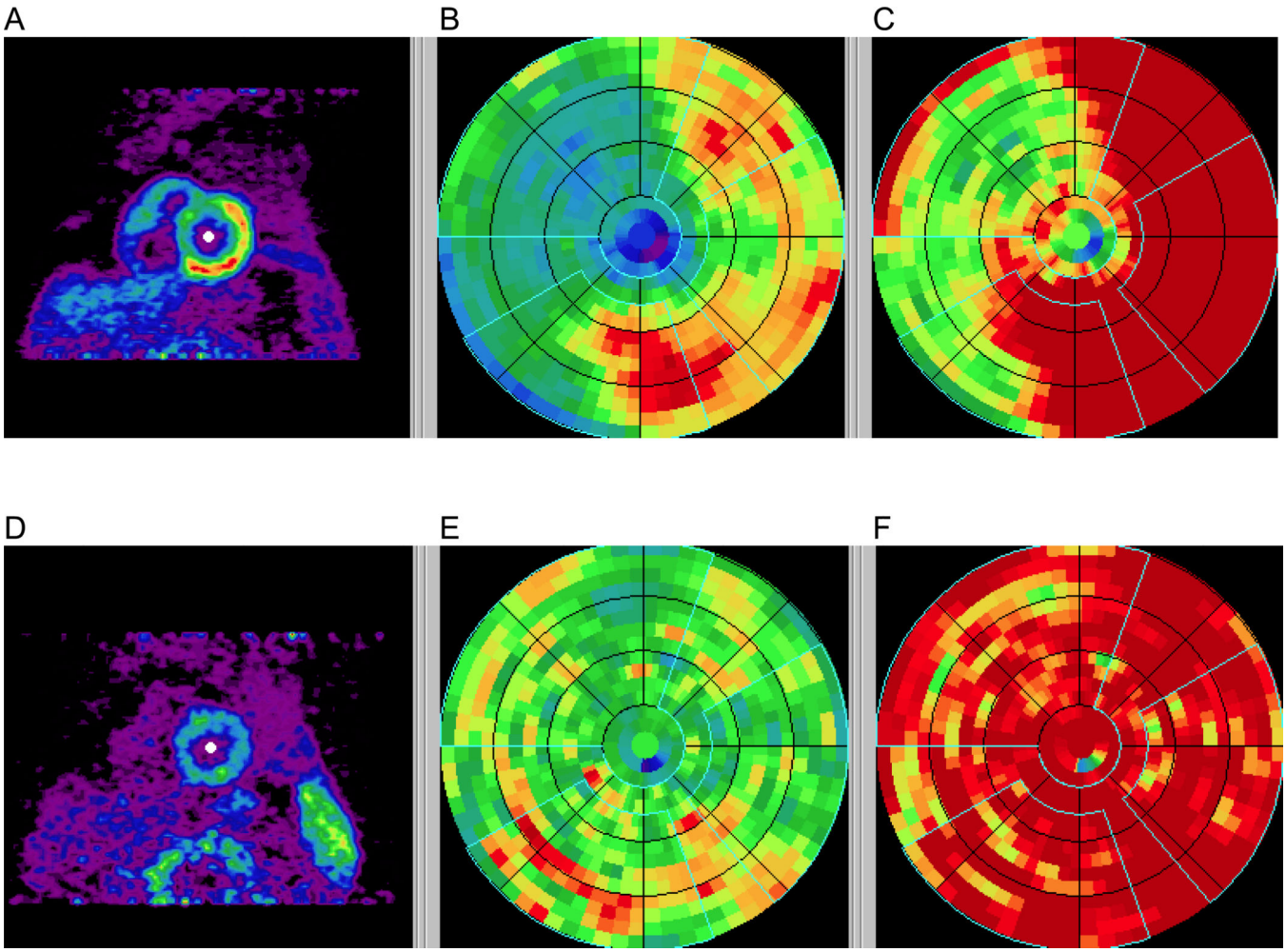

Figure 1.

Polar maps in a CAD patient with stress images (A–C) and rest images (D–F) demonstrating a reversible defect affecting mostly the LAD territory. Early summed images (0.5–2 min) were re-oriented into short-axis views (A, D), polar maps generated (B, E), and normalized based on averages of normal subjects (C, F). The vascular territories and the left ventricular chamber were defined on the polar map automatically.

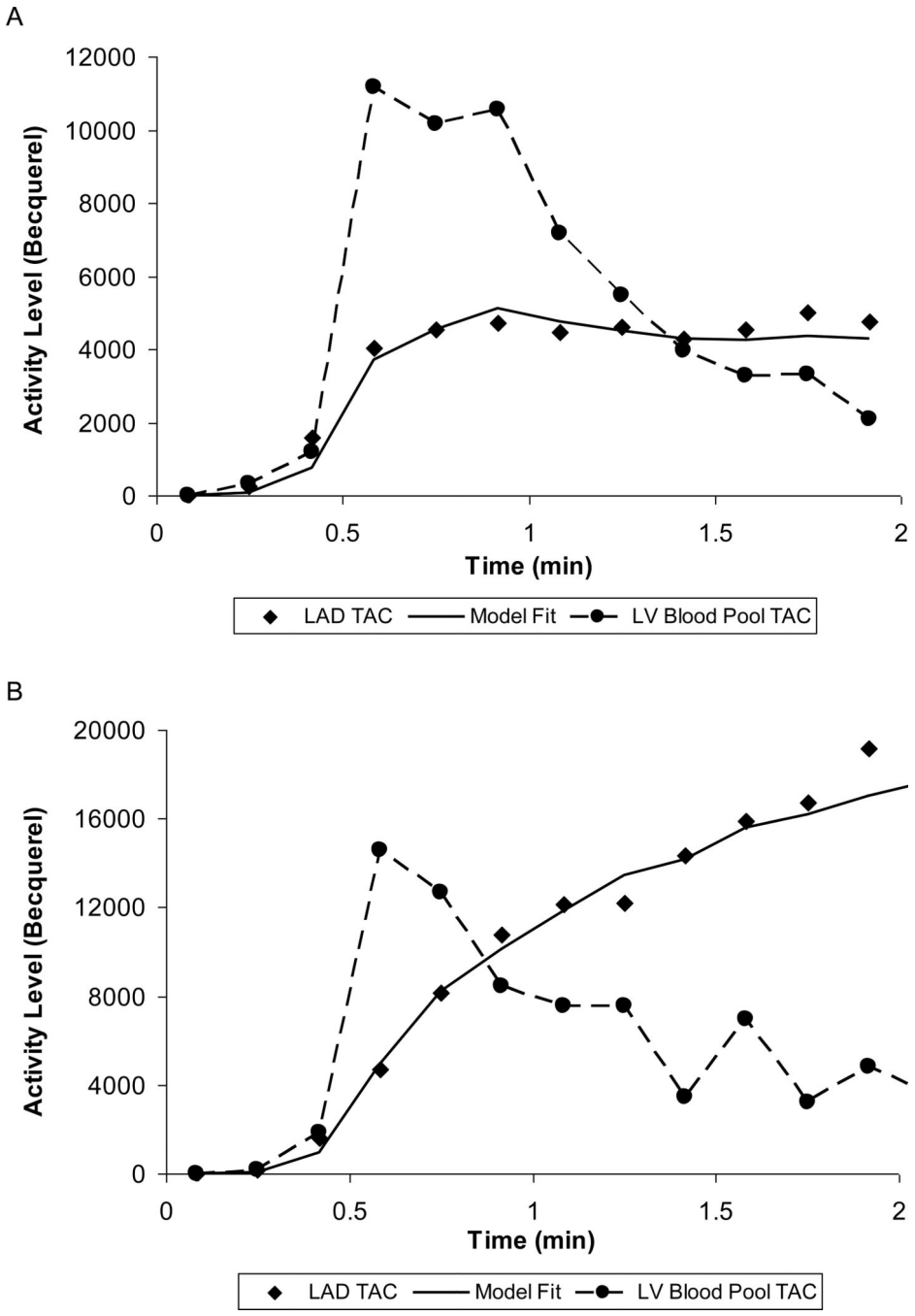

Figure 2.

Left ventricular blood pool time-activity curve (TAC) (circle symbols) and Left Anterior Descending Artery TAC (lozenge symbols) obtained from predefined vascular ROI on the polar map during rest (A) and with adenosine stress (B) in a normal subject. The solid curve is the model fit to the vascular territory myocardial TAC based on a single-compartment model.

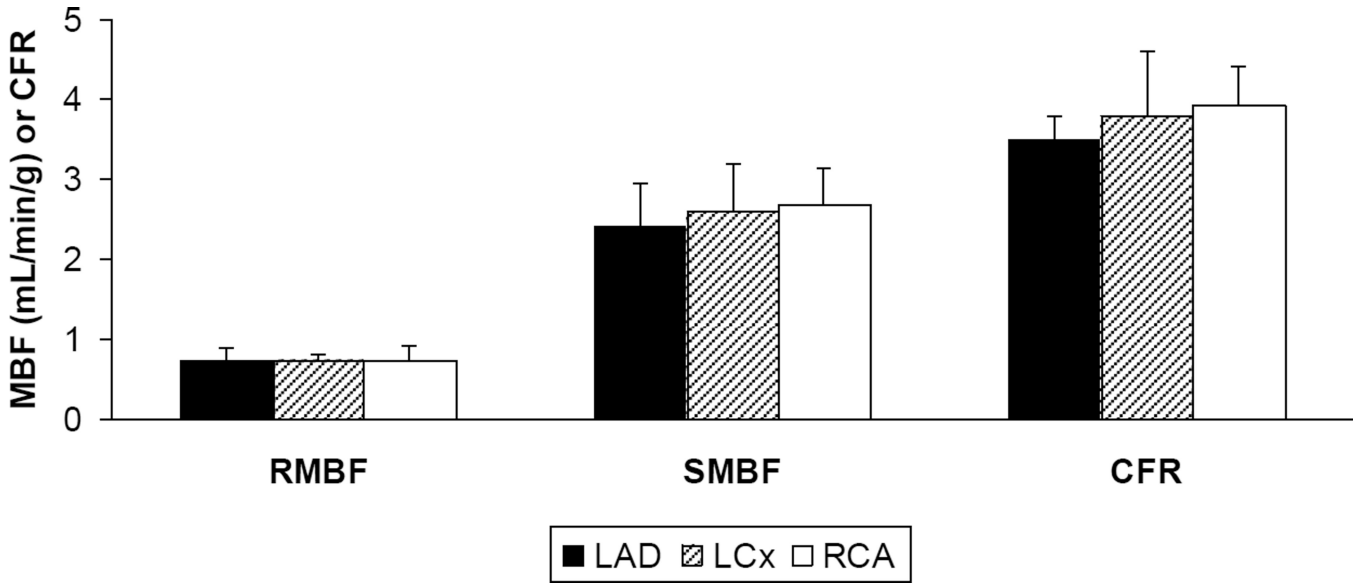

Figure 3.
Regional MBF at rest (RMBF) and during adenosine stress (SMBF) and MFR in the 3 vascular territories of normal subjects.

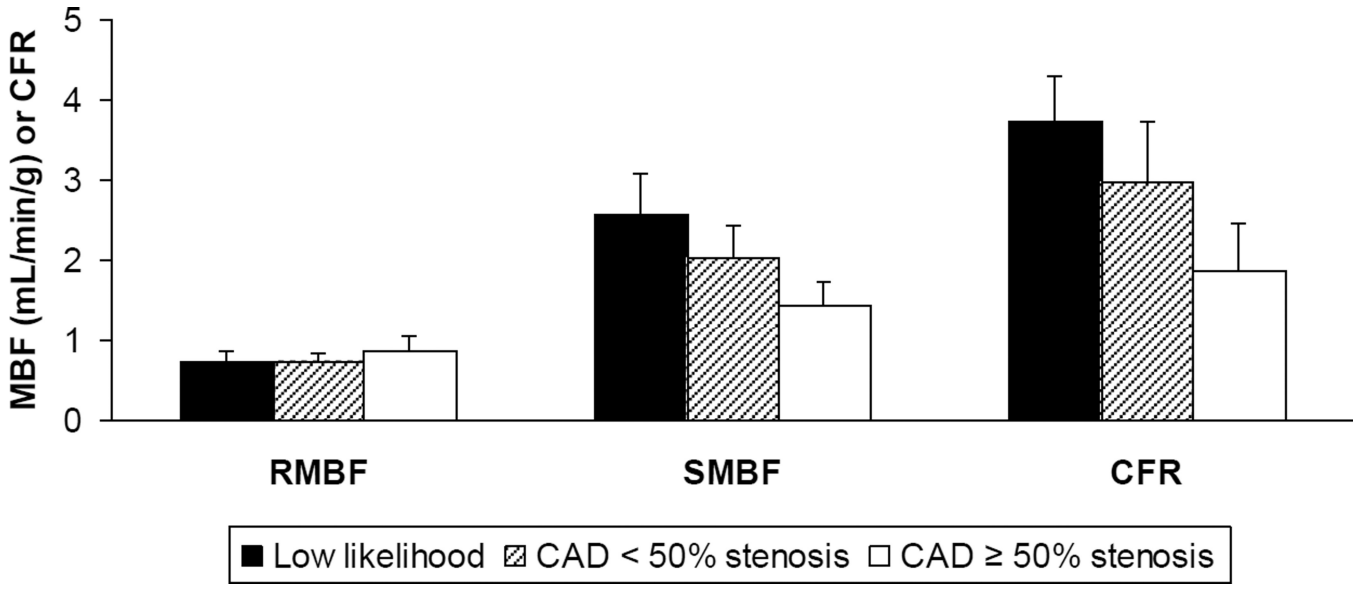

Figure 4.

Regional MBF at rest (RMBF) and during adenosine stress (SMBF) and MFR in vascular territories of normal subjects with low likelihood of myocardial ischemia vs. vascular territories of CAD patients with < 50% stenosis and ≥ 50% stenosis.

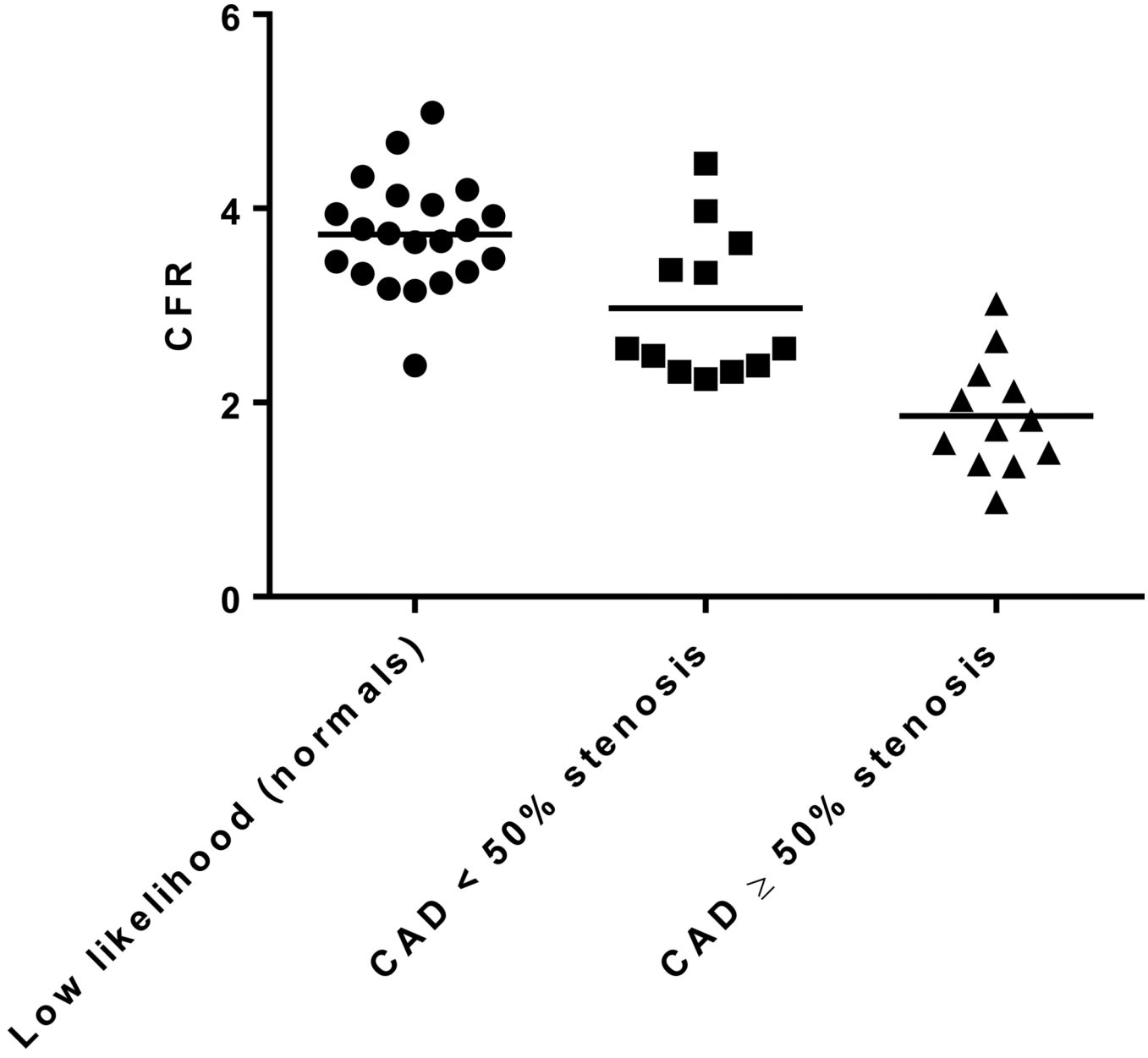

Figure 5.

Scatterplot of the MFR obtained from each individual territory in normal subjects with low likelihood of myocardial ischemia vs. CAD patients with < 50% stenosis and ≥ 50% stenosis.

Table 1

Baseline characteristics of normal subjects with low likelihood of myocardial ischemia and CAD patients

	Normal subjects (n = 7)	CAD patients (n = 8)
Age (years)	66	68
Sex (%)		
Male	86	100
Female	14	0
BMI (kg/m^2)	28	27
Cardiovascular risk factors (%)		
Hypertension	43	75
Diabetes mellitus	0	50
Dyslipidemia	71	88
Tobacco use - current	0	0
Tobacco use - former	43	75
Tobacco use - never	57	25
Labs (mg/dL)		
LDL	97	86
HDL	52	44
Creatinine	1.0	1.0
Medications (%)		
Antiplatelet agent	86	88
Statin	71	88
ACEI/ARB	43	63
Betablocker	57	75

Values are expressed as means or percentages.

CAD: coronary artery disease. LDL: low density lipoprotein. HDL: high density lipoprotein. ACEI: angiotensin converting enzyme inhibitor. ARB: angiotensin receptor blocker.

Table 2

MBF and MFR in vascular territories characterized by low likelihood of myocardial ischemia, < 50% stenosis and ≥ 50% stenosis.

	Low likelihood (n=21 territories from 7 subjects)				< 50% stenosis (n=12 territories from 8 patients)	≥ 50% stenosis (n=12 territories from 8 patients
	LAD	LCx	RCA	Global		
RMBF	0.73 ± 0.15	0.73 ± 0.09	0.74 ± 0.17	0.73 ± 0.13	0.73 ± 0.09	0.86 ± 0.21
SMBF	2.41 ± 0.54	2.58 ± 0.60	2.67 ± 0.46	2.53 ± 0.48	2.02 ± 0.40	1.43 ± 0.31
MFR	3.50 ± 0.29	3.77 ± 0.82	3.93 ± 0.47	3.70 ± 0.39	2.97 ± 0.76	1.86 ± 0.59

Values are expressed as means ± standard deviation.

RMBF: rest MBF. SMBF: adenosine stress MBF. MFR: myocardial flow reserve.